Interaction of free oscillating flat plate and VIV of a circular cylinder in laminar flow

Mohammad Jebelli, Mehran Masdari

Faculty of new sciences and technologies, University of Tehran, Tehran, Iran

Corresponding author: Mehran Masdari

Mailing address:

University of Tehran

Faculty of New Sciences and Technologies

North Kargar Street, Tehran, Iran

E-mail: m.masdari@ut.ac.ir

Abstract

The Flow-Induced vibration around bluff bodies is always of great interest in terms of control and suppressing the motion or amplifying and harvesting energy and the flat plates are known as useful means to make proper changes in flow structure. The objective of this paper is to investigate the effect of a downstream flat plate with one degree of freedom on the wake structure and FIV of an upstream circular cylinder in laminar flow. Numerical simulation is used to simulate the two-dimensional incompressible flow around two rigid objects with identical characteristic lengths and a variable horizontal spacing in a range of $0.5D \leq G \leq 4D$ to focus on the near wake and interaction of two objects. The results show that a free to vibrate flat plate located in the wake of a rigid cylinder not necessarily plays the role of a splitter in the near wake and starts to vibrate in an even small spacing such as $G=1.5D$. The Recirculation zone structure and its length are found to be the main reasons for induced vibration in such close configurations. In the case of simultaneous free oscillation, reducing the horizontal gap amplifies the amplitude of both objects. The interaction of the oscillating plate and the shear layers results in vortices with more strength that affect both objects. This amplification in oscillation amplitude shows that the present concept has a considerable potential to be utilized in the design of an improved energy harvesting system by converting fluid dynamic energy into electric energy from independent objects in a small area.

Keywords

Flow-Induced Vibration, Vortex Shedding, Circular Cylinder, Flat Plate, Low Reynolds Number

Introduction

The flow around bluff bodies has widespread applications in different industries and understanding its characteristics has been always of great interest. In some cases vortex formation and shedding, by changing the local pressure distribution around the body periodically, results in some types of flow-induced motions (FIMs). This periodic change comes with an asymmetric flow field and applies an oscillatory force which may induce a continuous motion to the objects located in the flow field. This oscillatory force can be either by the upcoming vortices that result in a wake-induced motion or buffeting or induced to the object by its own vortex shedding, which causes Vortex-induced Vibration (VIV) [1].

Lots of studies and reviews (such as Sarpkaya [2],[3]; Bearman [4]; Williamson and Govardhan [5]) have been performed to develop the knowledge and gain a better insight into different aspects of FIMs. The studies on FIMs can be divided into three main categories: understanding the phenomena, control and suppression, or enhance and amplifying the motion. Because of their destructive effects on structures, primitive studies were conducted to understand the phenomena and finding a way to suppress the vortex shedding and consequently the induced motions. On the other hand, global warming and other environmental problems have drawn attention to renewable energy sources in the past few decades. Harvesting energy from wind and current has been developed and a great deal of attention has been given to research in the field of FIMs as a clean and renewable energy source.

Different approaches are implemented to either suppress the FIMs to prevent structural damages or enhance them for harvest energy. An arrangement of a cylinder as a bluff body and an attached or detached flat plate has been extensively studied in the past decades. Although the primary studies were mainly focused on control induced motions, several attempts have been conducted to enhance them and to improve energy harvesting in recent years.

Early studies were devoted to find out the effect of a flat plate attached to the rear side of a fixed cylinder. In 1954 Roshko showed that the flat plate works as a splitter, stabilizes the wake, and delays the vortex shedding at a subcritical Reynolds number [6]. Change in vortex formation length and a lower Strouhal number are other results of this configuration found by Gerrard [7]. Apelt [8] found higher base pressure, lower drag and Strouhal number, and a narrower wake by stabilizing the separation point on the circular cylinder. The effect of a relatively short splitter plate (G<3D) in supercritical Reynolds numbers examined by Adachi [9] and a noticeable vortex suppression was observed. Kwon and Choi [10] studied the effect of the plate length in the laminar flow and concluded that attached splitters longer than a specific value completely suppress the vortex shedding. They also found that the Strouhal number rapidly decreases with increasing the length as long as G<1D.

Detached flat plates are also used to control the vortex shedding of cylinders. Ozono [11] studied the effect of detached splitter plate in subcritical Re numbers and found it useful to make a change in base pressure, Strouhal number, and even vortex shedding suppression. Its effectiveness is also reported to be connected to its both horizontal and vertical location. Hwang [12] observed similar behavior in laminar flow and introduced a critical horizontal spacing (G=2.6D) for maximum control efficiency. Akili [13] found that placing the splitter beyond 2D has no considerable effect on the cylinder. Dehkordi and Jafari [14] In an attempt to achieve maximum suppression showed that the critical horizontal spacing and the plate vertical location are significantly related. They also found that parallel splitters in proper location result in a diminution of 20% in the drag force.

Based on the studies mentioned above, it can be concluded that while both of the attached and detached plates can make a delay in vortex shedding and even a complete vortex suppression, the detached plates effectiveness are strongly more dependent on their length and location.

In 1990, Kawai studied the free vibration of a circular cylinder with an attached splitter plate. While this configuration prevents the shear layers to interact, the interaction between the flapping of the shear layers and the plate tip results in galloping with a high amplitude and low-frequency oscillation [15]. A bare circular cylinder can only be vortex-excited, but it can gallop in presence of a long stationary splitter plate with adequate length and this finding can be applied to any bluff body whether its cross section is sharp-edged or smooth [16]. Stapenbelt showed a transition from VIV to galloping with an increase in the plate length. The transition occurs in lower reduced velocities as the plate length increases [17]. Galloping with high oscillation amplitude is also reported by Assi and Bearman for a circular cylinder with a simple and slotted splitter[18]. On the contrary, Wu et al. found that a hinged plate could effectively suppress the VIV of a circular cylinder especially in low reduced velocities[19].

Liang et al. divided the cylinder response, based on the splitter length, into four groups: VIV, the interaction between galloping and VIV, a combination of the velocity-restricted excitation and interaction of VIV and galloping [20]. Sun et al. in an attempt to find the reason for the transition between VIV and galloping found that the lift components generated from the splitter and the cylinder behave, respectively, as the driving force and the suppressing force of galloping. Therefore it can be said that the transition is a result of competition between these forces [21]. A single downstream splitter alleviates VIV in low reduced velocities while exciting the galloping in higher velocities. On the other hand, an upstream splitter delays vortex shedding and makes the wake narrower. Zhu et al. also stated that using simultaneous oscillation can also suppress the galloping completely [22].

It can be concluded that using splitter plates to control the vortex shedding and flow-induced motions, whether attached or not, have different and even sometimes contradictory effects on the flow field and the cylinder behavior. Their length, rigidity, location, and type of connection to the cylinder are the main effective parameters.

In the past few years, some studies were focused on harvesting energy from different configurations of a cylinder and a plate. Installing an attached piezoelectric plate to the rear side of a cylinder has been investigated in different studies. An et al [23] proposed a novel vortex-induced piezoelectric energy converter (VIPEC) in which vortex-induced pressure difference acts on the plate and drives the plate to squeeze piezo patches to convert fluid dynamic energy into electric energy. They found that Different lengths of the plate change in shear layers interaction and delays vortex shedding. Wang et al. investigated the VIV of a piezoelectric cantilever plate located in the wake of a circular cylinder. They divided the gap between two bodies into two sections: suppression, vortex shedding and showed that this gap is related to the plate’s length [24]. Armandei and Fernandes [1] in 2016 tried to extract marine current energy through buffeting. They elastically installed a flat plate with rotational freedom in the wake of a modified D shape cylinder. They found buffeting response independent from the distance and the efficiency is dependent on the elastic axis position and the spring rate. These results show that while the wake of any bluff body can be considered as a source to harvest energy, utilizing a proper configuration is essential for higher efficiency.

From the studies reviewed above, it is known that while the flat plates are widely used to control and suppress the FIMs, they are also noticed as means to amplify the motion of the cylinder and even harvesting energy directly. On the other hand, small changes in the length, location, and degree of freedom may change the system response significantly. It seems there are still unknown aspects in the interaction of a plate and a circular cylinder.

In this work, the FIMs of a combination of a circular cylinder and a flat plate with one degree of freedom has been numerically studied in a laminar flow regime. The plate is located in the cylinder wake, and the gap spacing is defined as the distance between the trailing point of the cylinder and the leading edge of the plate. The objects are independent and each of them is able to oscillate in crossflow direction freely. This study aims at exploring the effects of horizontal spacing on the flow structure and system response when the plate oscillates individually or both objects oscillate simultaneously.

Nomenclature

A	Plunging Amplitude
D	Circular Cylinder Diameter
L_P	Flat Plate Length
G	Non Dimensional Horizontal spacing
m^*	Mass Ratio
ζ	Damping Factor
CL	Lift Coefficient
CL_{rms}	Root Mean Square of Lift Coefficient
CD	Drag Coefficient
Cp	Pressure Coefficient
Cp_b	Base Pressure Coefficient
f	Plunging Oscillation Frequency
f_n	Transverse Natural Frequency
ρ	Fluid Density
m	Body Mass
m_A	Added Mass
K	Transverse Stiffness Factor
U_{in}	Free Stream Velocity
U_r	Reduced Velocity
t	Physical Time
T	Non Dimensional Time

Problem description

The FIV of a circular cylinder and a flat plate located in the wake is modeled by a mass-spring system with one degree of freedom proposed by Facchinetti et al. [25]. Figure 1 presents the schematic view of flow past the objects which are elastically mounted perpendicular to the uniform flow. D and L_P represent the cylinder diameter and the plate's length respectively. The streamwise gap between the rear end of the cylinder the leading edge of the plate is shown by G=L/D. In all cases the length of the flat plate and the cylinder diameter are equal and the plate thickness is set as $\delta = 0.03D$.

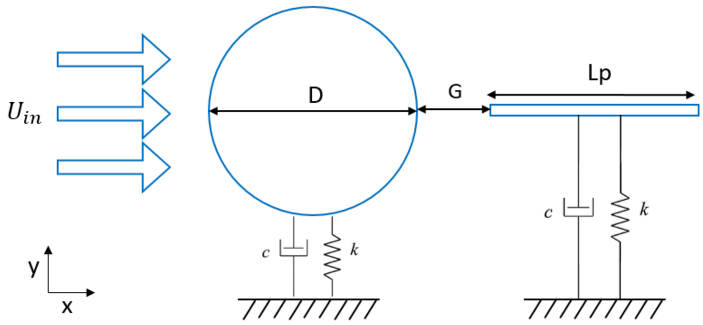

Figure 1 – schematic diagram of flow past a free to oscillate cylinder and flat plate in tandem arrangement

In FIV, the Reynolds number, the mass, and damping ratios play a significant role in the dynamic response of the system. The mass ratio is defined as $m^* = m/m_A$ based on the mass (m) of the body, and its added mass. Damping ratio can also be defined as $\zeta = c\ /\ (2\sqrt{mk})$, where C and K are the damping and spring stiffness of the system. Williamson [26], [27] reported that the wake transition of a circular cylinder occurs when Re is larger than 180, which was confirmed by Jiang et al. [28]. The two-dimensional (2D) simulations were performed at Re = 100 for all cases to avoid the flow three dimensionality effects. As the main goal of the current study is to find out the effect of different horizontal spacing on the behavior of the system, the mass ratio and Re number are kept constant at 10 and 100, respectively. The structural damping is also set to zero (ζ = 0) to encourage a high amplitude of oscillation. The natural frequency of the system is also set based on the Strouhal number and vortex shedding frequency of a bare fixed circular cylinder. Table 1 summarizes the main parameters for simulation where U_r is the reduced velocity and can be defined as $U_{in}/f_n D$.

Parameter	symbol	value
Mass ratio	m*	10
Damping ratio	ζ	0
Horizontal space	G=L/D	0.5-0.4
Reynolds number	Re	100
Reduced velocity	U_r	6

Table 1 – Main Simulation Parameters

Governing equations

Based on the above assumptions, the flow over the objects is governed by the 2D incompressible unsteady Navier–Stokes (NS) equations. The conservation of mass and momentum, therefore, is given as follows:

$$\frac{\partial u^*}{\partial x^*} + \frac{\partial v^*}{\partial y^*} = 0, \qquad (1)$$

$$\frac{\partial u^*}{\partial t^*} + u^* \frac{\partial u^*}{\partial x^*} + v^* \frac{\partial u^*}{\partial y^*} = -\frac{\partial p^*}{\partial x^*} + \frac{1}{Re}\left(\frac{\partial^2 u^*}{\partial x^{*2}} + \frac{\partial^2 u^*}{\partial y^{*2}}\right), \qquad (2)$$

$$\frac{\partial v^*}{\partial t^*} + u^* \frac{\partial v^*}{\partial x^*} + v^* \frac{\partial v^*}{\partial y^*} = -\frac{\partial p^*}{\partial y^*} + \frac{1}{Re}\left(\frac{\partial^2 v^*}{\partial x^{*2}} + \frac{\partial^2 v^*}{\partial y^{*2}}\right), \qquad (3)$$

In equations (1), (2), and (3), the dimensionless variables are evaluated as follows:

$$x^* = {}^{x}/_{D} \quad y^* = {}^{y}/_{D} \quad u^* = {}^{u}/_{U_{in}} \quad v^* = {}^{v}/_{U_{in}} \quad p^* = {}^{p}/_{\rho U_{in}{}^2} \quad t^* = {}^{t}/_{U_{in} D}$$

In the above equations, u and v stand for the velocity components in x- and y-directions, respectively, t is the flow time, ρ is the fluid density, U_{in} is the flow inlet velocity, D is cylinder diameter and p represents the static pressure of the fluid.

The mechanical response of the mass-spring-damper model is governed by the corresponding equation of motion as:

$$m\ddot{Y} + 2m\zeta\omega_0\dot{Y} + m\omega_0^2 Y = f_l(t) \qquad (4)$$

Where Y, $\dot{Y}$ and $\ddot{Y}$ denotes the transverse displacement, velocity, and acceleration of the structure respectively. $\omega_0 = 2\pi f_n$ is the natural circular frequency of the system and $f_l(t)$ is the time dependent lift force acting on the subject.

Numerical method

The flow field in the current study is numerically simulated with reliable CFD software ANSYS Fluent. In the case of FIV simulations, as the subject oscillates, a dynamic mesh is required to change the grid in every time step. ANSYS Fluent employs an Arbitrary Lagrangian-Eulerian (ALE) algorithm which includes three dynamic mesh schemes, namely, smoothing, layering, and remeshing. A diffusion-based smoothing method is used in the current study and a User-Defined Function (UDF) is also employed using the C Programming Language to solve the system's response in FIV.

In numerical simulations, the size of the computational domain and especially the blockage effect are of great importance and small domains may result in errors in the prediction of the forces and system behavior. On the other hand, a vibrating cylinder, Compared to a stationary one, is associated with a wider wake and consequently, the blockage is expected to play an even more significant role.

Prasanth and Mittal showed that for a circular cylinder in laminar flow ($m*$= 10, Re =100) blockage of more than 2.5% can lead to hysteresis in the response of the cylinder at the onset of synchronization. It also leads to an error in the prediction of aerodynamic forces [29], [30].

They also studied the VIV of two circular cylinders in tandem and staggered arrangements and located the lateral boundaries in 25D from the upstream cylinder which results in a blockage of 2% [31].

The size of the flow domain, the geometry of the model, and the boundary conditions of the current study are presented in Figure 2. The center of the cylinder is the origin of the coordinate system and the size of the whole computational domain is 75D×50D. The upstream and lateral boundaries are located 25D from the center of the cylinder and the downstream boundary is located 50D from the origin to capture the wake accurately.

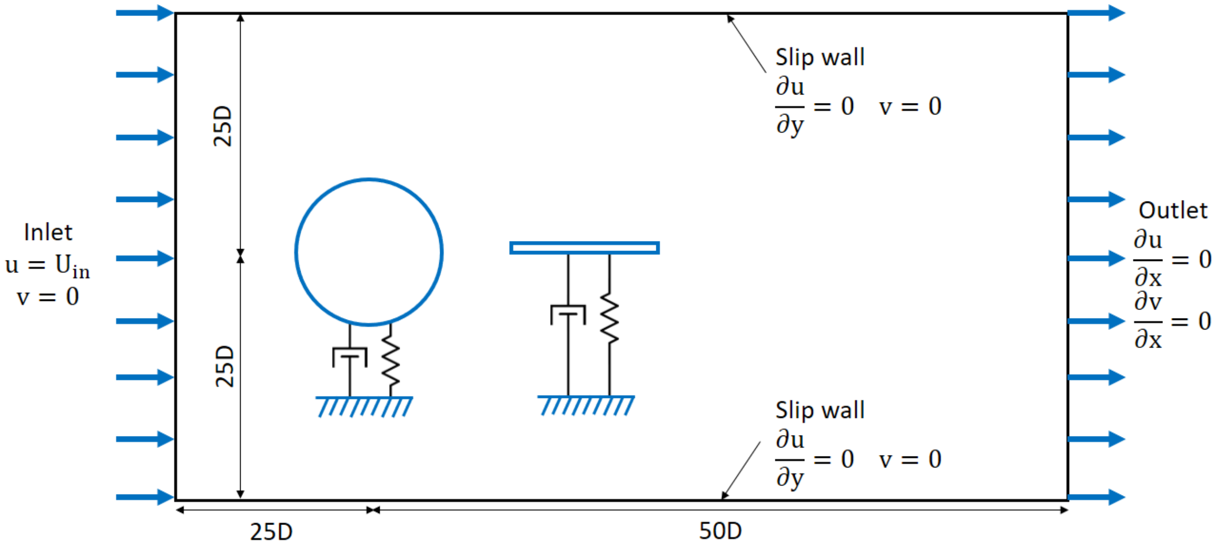

Figure 2 – The flow simulation domain, Geometry of the model and boundary Condition

The surface of the cylinder and the plate are assumed to be smooth, with a no-slip boundary condition ($u = 0$, $v = 0$). The inlet boundary is imposed with a uniform velocity boundary ($u = U_{in}$, v = 0). The top and bottom boundaries are prescribed with the normal component of the velocity and component of the stress vector along the boundary equal to zero (∂u / $\partial y = 0$, $v = 0$). Finally, the zero normal gradient condition for velocity is assigned in the outlet and the pressure is specified as a reference value of zero (∂u / $\partial x = 0$, ∂v / $\partial x = 0$, p = 0).

Computational domain and mesh dependency

In the first step, before conducting a detailed study on the main case, mesh independence and temporal resolution validation are performed to achieve an independent solution method.

Figure 3 shows the grid generated for the simulation of flow filed around a circular cylinder and a downstream flat plate. In all of the cases the mesh around the cylinder's surface has been divided into four sections: front, up and down and finally the rear side which the last one is more important due to the presence of the plate and high flow gradients. The mesh is also gradually coarsened to decrease the computational cost in regions far away from the structures.

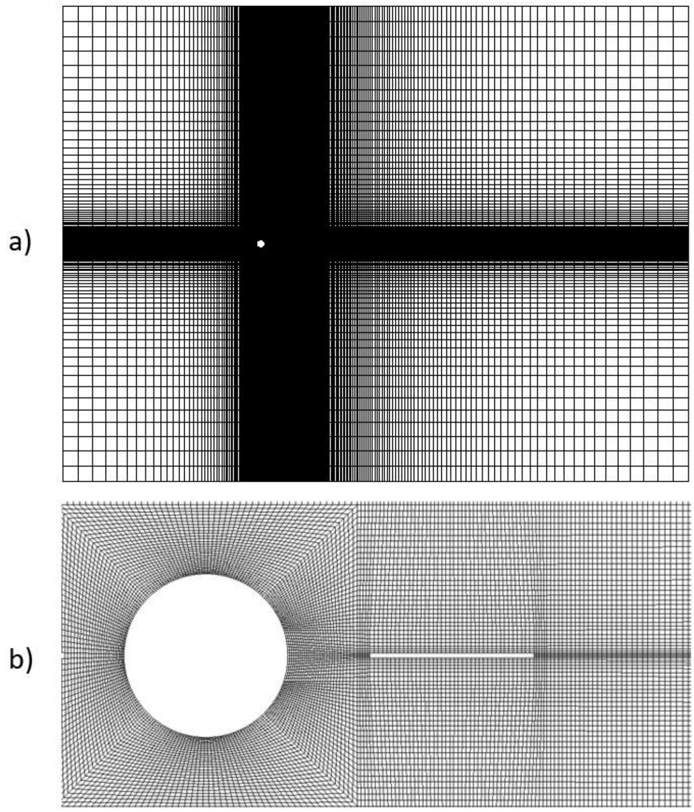

Figure 3 – Grid distribution: a) around the cylinder and plate, b) the whole grid system

The grid dependency study has been conducted on two configurations including the 2DOF VIV of a bare circular cylinder and a fixed cylinder with a flat plate in the wake (G=3D). The grid's structures are generally similar, but for the latter case, due to the presence of the plate, there are more cells in the wake.

For the first case, it can be seen that the variations of the normalized mean in-line and the maximum cross-flow amplitudes, the Strouhal number, and the mean drag coefficient converge in case G-1-2 with 200 nodes equally distributed on the cylinder surface (Table 2).

Grid	Nodes on the cylinder	X_{mean}	Y_{max}	St	Cd_{mean}
G-1-1	4×40	0.116	0.656	0.1634	1.986
G-1-2	4×50	0.115	0.647	0.1635	2
G-1-3	4×60	0.1151	0.645	0.1635	1.997

Table 2 - Grid independency study for 2D VIV of circular cylinder (Re=100, Ur=6.02)

Table 3 presents the results of the second case. A grid with 40% more cells in rear side of the cylinder (G-2-3), assures that the results are independent from grid resolution.

Grid	Nodes on cylinder	Cylinder				Flat Plate			
		Cl_{max}	Cl_{rms}	St	CD_{mean}	Cl_{max}	Cl_{rms}	St	CD_{mean}
G-2-1	3×50+50	0.41	0.288	0.157	1.311	1.245	0.87	0.157	0.0782
G-2-2	3×50+60	0.405	0.288	0.157	1.310	1.254	0.875	0.157	0.0795
G-2-3	3×50+70	0.405	0.286	0.157	1.310	1.257	0.883	0.157	0.0799
G-2-4	3×50+80	0.405	0.285	0.157	1.309	1.258	0.884	0.157	0.0798

Table 3 - The grid independence test for a stationary cylinder and a flat plate 3D downstream at Re=100

According to the results, the grid G-2-3 is selected for further simulations on a fixed or oscillating combination of a cylinder and a flat plate. In the second test, for the temporal resolution analysis, the mesh G-2-3 is examined for several time steps and a non-dimensional time step of $\Delta t = 0.002$, is found to be sufficiently small to assure independency.

Model validation

This section aims to provide a validated computational approach to simulate the flow field around stationary and oscillating subjects. Three cases including a stationary/oscillating cylinder and a fixed cylinder with a flat plate in the wake are simulated and the results are compared with previous studies. All the cases have a similar simulation domain which is described before. In Table 4 the aerodynamic characteristics of the flow around the stationary cylinder at Re=100 are compared with previous studies. The good agreement shows that the current simulation approach is capable of predicting the case with acceptable accuracy.

Author	**CD_{mean}**	**St**	**CL_{rms}**	**$-Cp_b$**
Park et al. (1998) [32]	1.33	0.165	0.235	0.725
Kravchenko and Moin [33]	1.32	0.164	0.222	0.73
Shi et al. [34]	1.318	0.164	-	-
Mittal [35]	1.322	0.1644	0.226	-
Stalberg et al. [36]	1.32	0.166	0.233	-
Posdziech and Grundmann [37]	1.325	0.1644	0.228	0.709
Li et al. [38]	1.336	0.164	-	0.701
Qu et al. [39]	1.319	0.1648	0.225	0.709
Present study	1.34	0.165	0.232	0.71

Table 4 - Comparison of flow quantities with published results for flow around a stationary cylinder at Re= 100

For the second case, the variation of Strouhal number and Drag coefficient of the circular cylinder and a wake mounted splitter plate is presented in Figure 4 and Figure 5.

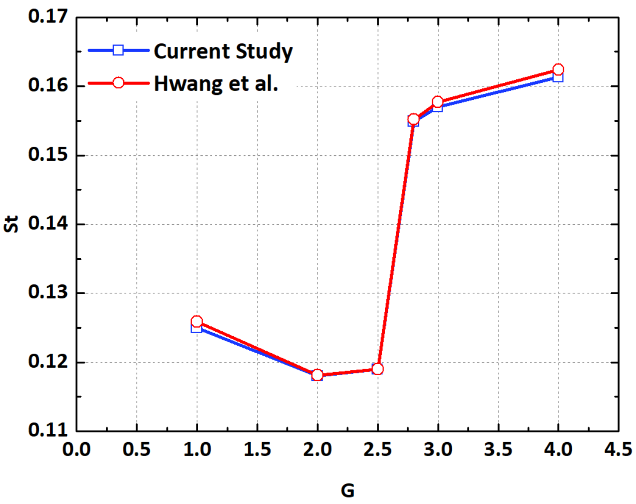

Figure 4 - Variation of Strouhal number for different spacing in Re=100 [12]

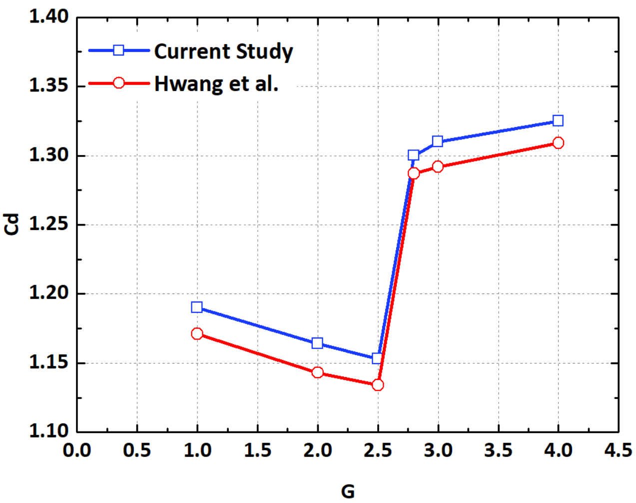

Figure 5 - Variation of drag coefficient for different spacing in Re=100 [12]

The results of the current simulation are in agreement with those of Hwang et al [12]. The plate changes the wake structure for L/D≤2.5 and decreases the drag coefficient and Strouhal number significantly. For L/D≥2.8, a regular vortex shedding appears and both of the parameters jump to higher values. To examine the accuracy of the numerical method to simulate the 2DOF VIV, the results of the current simulation are compared with some earlier studies in Table 5.

Author	Y_{max}	X_{mean}	St	CL_{max}	CD_{mean}	CD_{rms}
Prasanth and Mittal (2008) [30]	0.53	0.1115	0.1643	0.1929	1.90	0.2486
He et al. (2012) [40]	0.503	0.1082	0.1652	0.1985	1.81	0.2244
Tu et al.(2015) [41]	0.525	0.1307	0.1652	0.2220	1.88	0.2664
Present study	0.54	0.110	0.1640	0.235	1.88	0.2660

Table 5 - Comparison of the results of the current study with previous studies for 2D VIV of a circular cylinder at Re= 100 and Ur=6

The good agreement confirms that the reliability of the numerical approach. Figure 6, presents the variation of maximum amplitude of the cylinder for a range of Re numbers. It can be seen that the results agree well with those of Prasanth and Mittal [30] (Decreasing case) and Tu Et al. [41].

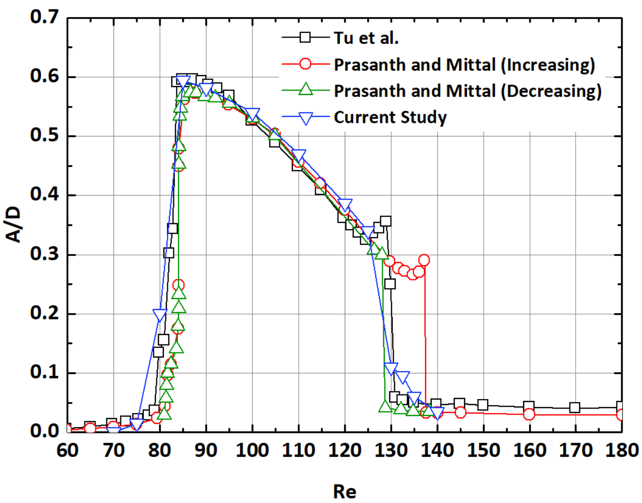

Figure 6 - Variation of statistical values of the cylinder responses with Re (Transverse oscillation amplitude)

Oscillation amplitude follows the trend; the maximum amplitude has been predicted well and there is only little differences in the beginning and end of synchronization regime.

Considering all the differences mentioned above, it can be concluded that the present numerical approach is able to predict the FIV of a cylinder and a downstream flat plate with adequate accuracy.

Results

The results of the current study are divided into two parts. In the first one, the flow field and the response of a flat plate with one DOF in cross flow direction that is located in the wake of a stationary circular cylinder are presented. The second part deals with simultaneous free vibration of the circular cylinder and the plate and the interaction of two objects in small horizontal spacing.

Stationary cylinder, Vibrating flat plate

According to the previous studies the location of the flat plate has a significant effect on the vortex formation and the wake structure. Therefore 10 different configurations in a spacing range of 0.5D<G<4D have been numerically simulated. The cylinder diameter and the flat plate's length are equal and all the simulations are conducted at a Re number of 100 which is equivalent to a reduced velocity of 6.

A fixed flat plate located in the wake of a stationary cylinder can perform as a splitter and delays or even suppress the vortex shedding depending on its location [12]. This behavior is a result of changing the recirculation zone (R-Z) on the rear side of the cylinder. Based on the current simulations, the system response for a flat plate with a 1DOF in transverse direction is different. The vibration amplitude and frequency ratio of the flat plate in different configurations are presented in Figure 7:

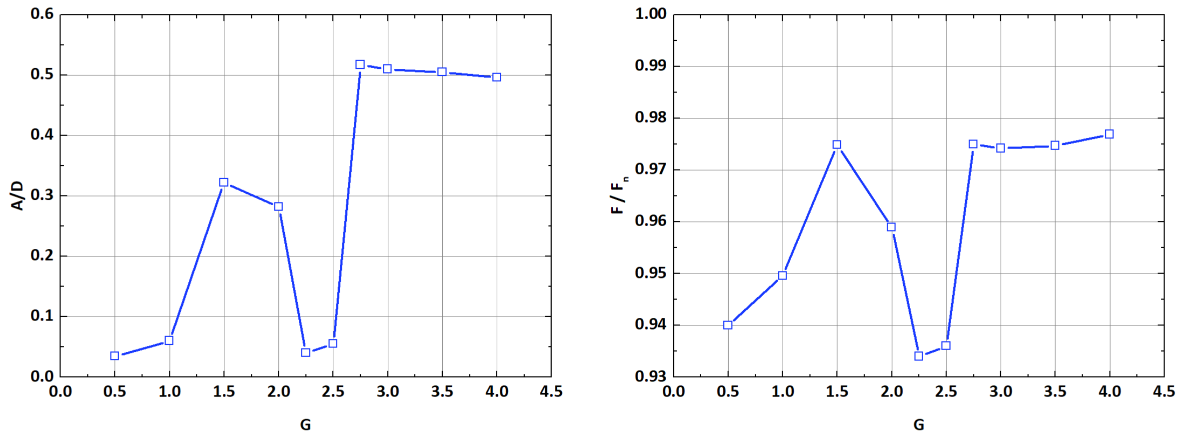

Figure 7 – Oscillation amplitude (Left) and frequency ratio (Right) of the flat plate located in the wake of a stationary cylinder

Flat plates which are located outside of a critical distance from the rear end of the cylinder, about 2.6D and introduced by Hwang [12], show an anticipated behavior and oscillates sinusoidally. It oscillates beyond this critical distance, because of adequate space for vortices to form and shed into the wake. Therefore the plate faces with a local asymmetric pressure field and starts to vibrate. In this condition, as it approaches the cylinder, due to facing stronger vortices, the oscillation amplitude slightly increases up to A/D=0.517 for G=2.75D.

The system response is just similar to that of a fixed plate for G=2.25D and G=2.5D and the vibration almost vanishes. While the frequency ratio follows the natural frequency of the fixed cylinder for G≥2.75, it gets far from it in this region.

Smaller spacing interestingly results in higher vibration amplitude, although it is about 50% less than those of G=2.75-4D. When the spacing sets as G=0.5-1D the flat plate rolls as a splitter and both of the amplitude and frequency fall again.

Generally, the vibration amplitude in the crossflow direction and the variation of lift force are relevant. In Figure 8 the variation of Cl_{rms} of the flat plate for different configurations are presented and compared with those of a fixed one.

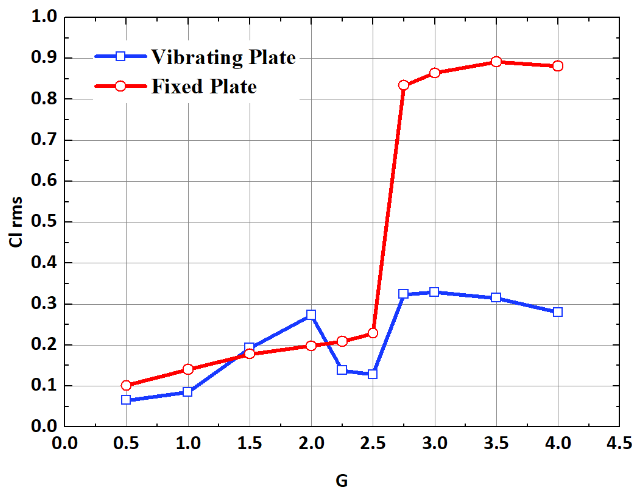

Figure 8 – Variation of CL_{rms} of the flat plat in different configurations

For large horizontal spacing (G≥2.75), the oscillation of the plate and change in its position results in considerably lower Cl_{rms} than that of a fixed one. The lift force falls in G=2.5D for both of the fixed and free plates. As expected, this coincides with the vanishing of the vibration. While the force decreases gradually for the fixed plate, there is a temporary growth for the cases with G=1.5, 2D which once again has similar behavior to the vibration amplitude. The Cl_{rms} falls again for smaller spacings.

This system response is related to the near wake flow field and as mentioned before, the R-Z has a significant effect on its structure and vortex shedding pattern. Figure 9 presents the variation of this region in different configurations:

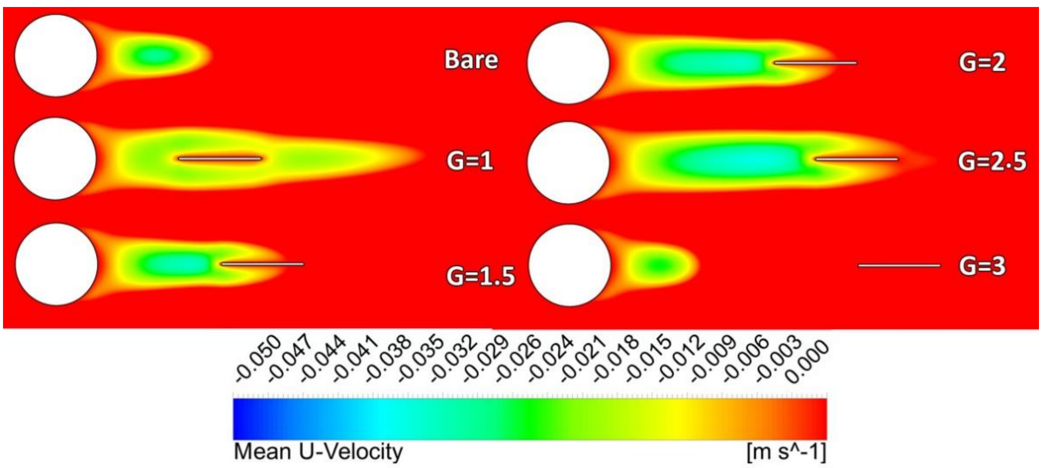

Figure 9 –Recirculation zone of a bare cylinder and the effect of free to oscillate flat plate in different configurations

The presence of the flat plate with 1DOF changes the R-Z in a way which is different to that of a fixed one presented by Hwang [12]. For G=1D, the recirculation length growths significantly, and the plate is entirely confined to this region. When the plate is placed slightly further (G=1.5, 2D), a shorter R-Z appears and a small part of the plate is outside of it. In the case of G=2.5D, a larger R-Z appears that is stretched up to the trailing edge of the flat plate. Larger horizontal spacing (G≥3D) results in a short R-Z which is similar to that of a bare one. Comparing the R-Z, the plate location and vibration amplitude shows that the plate starts to vibrate with a considerable amplitude only in cases that the plate is not entirely surrounded by this region.

In the case of G=3D, the plate which is located completely outside of this region faces shedding vortices and consequently has a considerable vibration amplitude. The vibration mechanism for G=1.5, 2D , in which the R-Z is larger and no regular vortex shedding has been formed before the plate, is different. To achieve a better understanding of this mechanism, a closer look into the wake structure for different configurations might be beneficial. Figure 10 shows the streamlines in near wake of the cylinder for an identical moment ($Cl_{cylinder}$=0). A regular vortex shedding pattern of a bare cylinder is also presented for a better comparison.

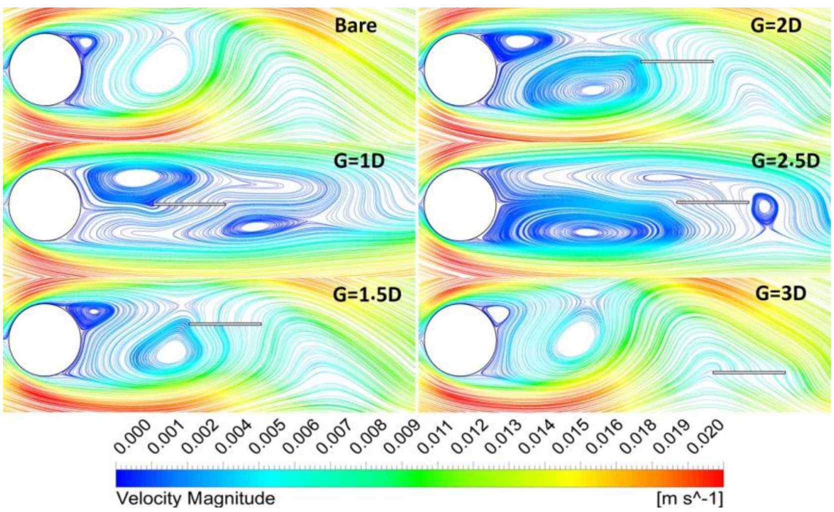

Figure 10 – Comparison of the wake structure in different configurations

When the plate is placed in G=1D, unlike the bare cylinder, Large and stretched vortices are generated that surround both the upper and lower sides of the plate. This flow structure confirms the large R-Z and may explain the reason for low vibration amplitude due to low pressure difference. For G=1.5, 2D, the wake structure is somehow similar to the case of a bare cylinder and the vortices form and move downstream periodically. As the plate goes further (G=2.5D), once again large and stretched vortices appear that are even larger than those of G=1D. These large structures are matched with the growth of R-Z. Placing the plate in further locations (G≥3D) results in a near wake similar to a bare cylinder. A regular vortex shedding pattern appears and the vibration is based on the interaction of the plate and the vortices which are completely formed and move downstream periodically. Instantaneous streamline contours at equal intervals are presented in Figure 11 during one cycle of plate vibration for three configurations.

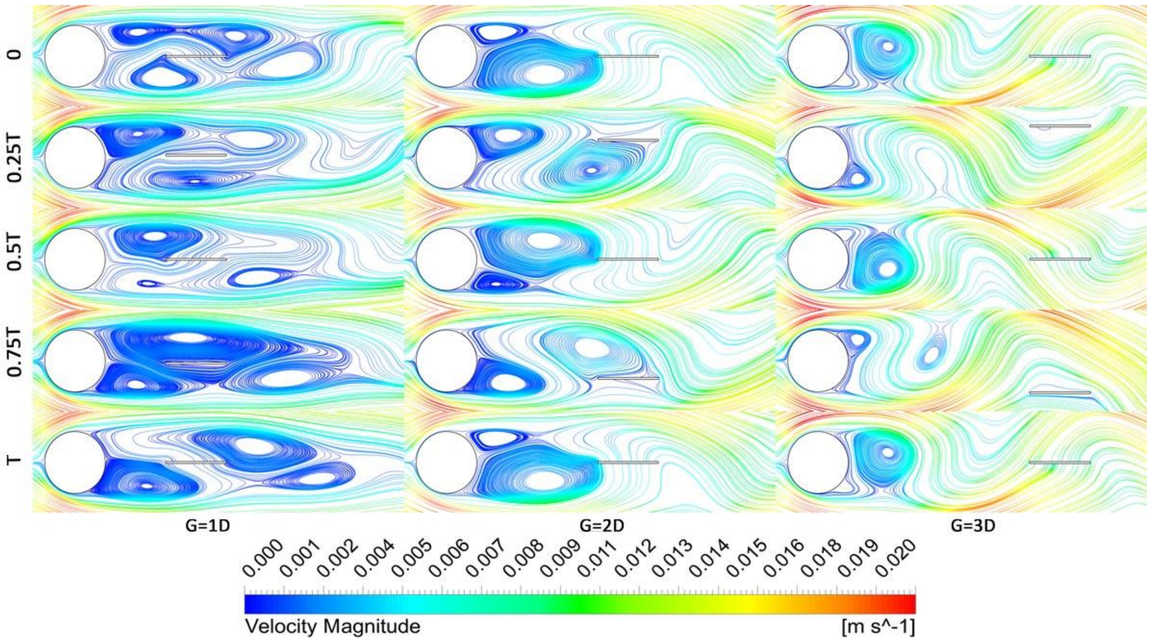

Figure 11 – Wake structure during one cycle of plate oscillation for cases G=1D, G=2D, G=3D

When the plate is located at G=1D, the lack of interaction between two shear layers, changes the R-Z structure and formation of each vortex is based on the same side shear layer and results in large and stretched vortices. As the plate goes further (G=2D), a familiar wake structure can be observed with a periodic vortex formation. In each side, the vortex grows up to the plate's leading edge, separates from the cylinder by the shear layer of the opposite side and finally moves downstream which creates an asymmetric flow field around the plate . This mechanism is almost similar to that of a bare cylinder or a cylinder and a plate which is located far enough (G=3D). The main difference between the cases G=2, 3D is in the larger size of the vortices for the first one.

Figure 12 presents the velocity magnitude and the spanwise vorticity contours of the flow field for cases G=1, 2, 2.5, 3D in an identical moment (Y_{plate}=0).

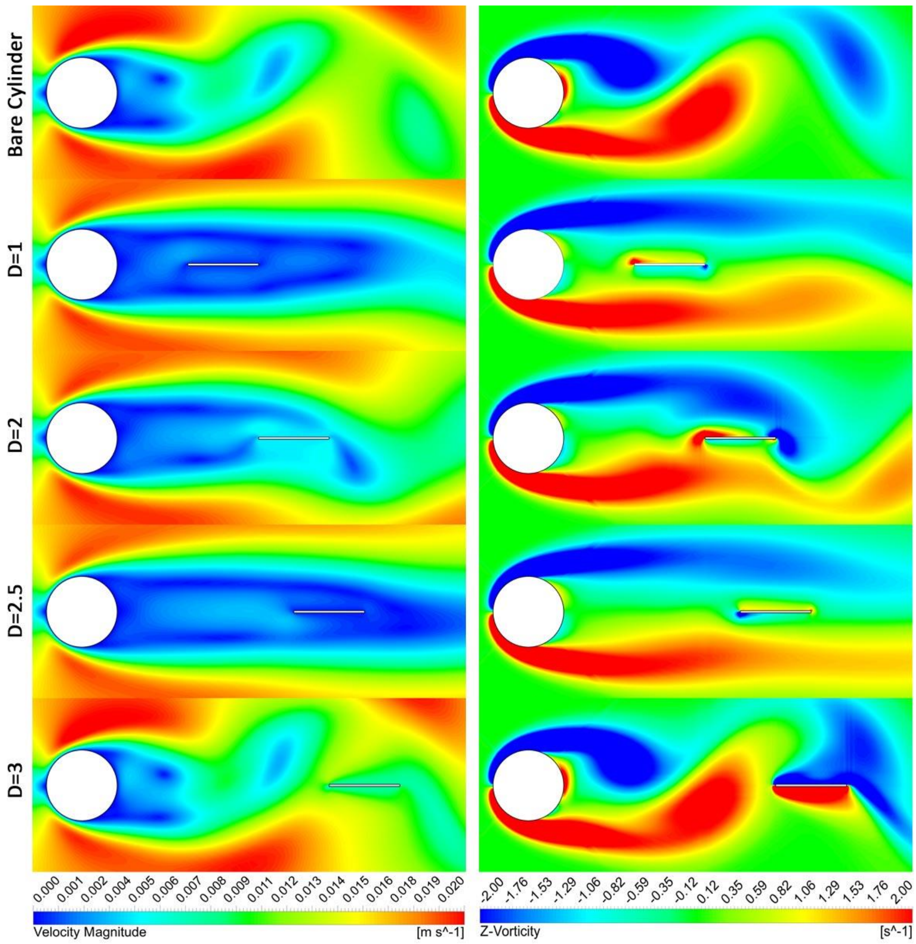

Figure 12 – Velocity magnitude and spanwise vorticity contours in different configurations (Y_{plate}=0)

For the case of G=1D, the near wake includes two separated shear layers and the plate is entirely covered by the R-Z with a low velocity magnitude. In this case, the cylinder and the plate can be considered as a whole body. A periodic vortex formation occurs just before the plate with a larger gap in case G=2D. This mechanism results in an asymmetric flow field around the plate surface and consequently, it starts to vibrate. Due to the presence of the plate, the vortex shedding occurs further downstream when they just have passed the trailing edge of the plate. In the case of G=2.5D, the objects just behave as a whole body, and a similar pattern to the case G=1D can be seen. This Larger gap also delays the start of vortex shedding even further downstream. In the last case, there is enough space for a fully formation and shedding of the vortices. The flow pattern and vibration mechanism are similar to that of a bare cylinder.

Simultaneous FIV of the cylinder and the flat plate

The results of simultaneous FIV of a cylinder and a flat plate in tandem arrangement are presented in this part. All of the configurations and simulation parameters are similar to the last part. It is necessary to mention that the term (bare oscillation/vibration) deals with the FIV of a single and bare object in the flow field and the term (individual oscillation/vibration) indicates the FIV of one object while the other object is stationary which indicates the results of last section.

The oscillation amplitude and frequency ratio of the cylinder are presented and compared to those of a bare cylinder in Figure 13:

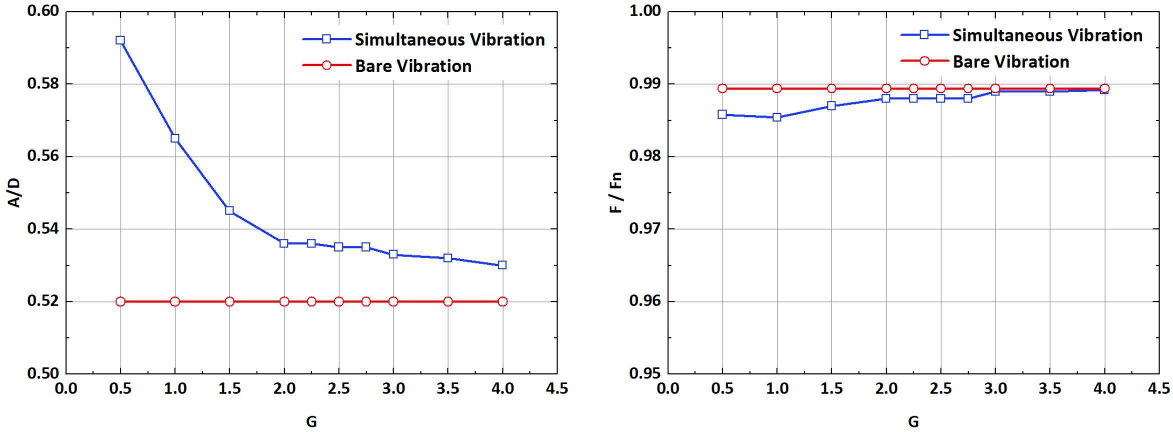

Figure 13 – Oscillation amplitude (left) and frequency ratio (right) of the bare cylinder and the cylinder in simultaneous vibration

The oscillation amplitude is slightly higher in simultaneous vibration than that of the bare cylinder for large gaps. As the spacing decreases, the amplitude grows gradually and reaches up to A/D=0.592 for the case of G=0.5D which is about 14% higher than the bare cylinder. The frequency ratio is almost constant and follows system’s natural frequency for all cases.

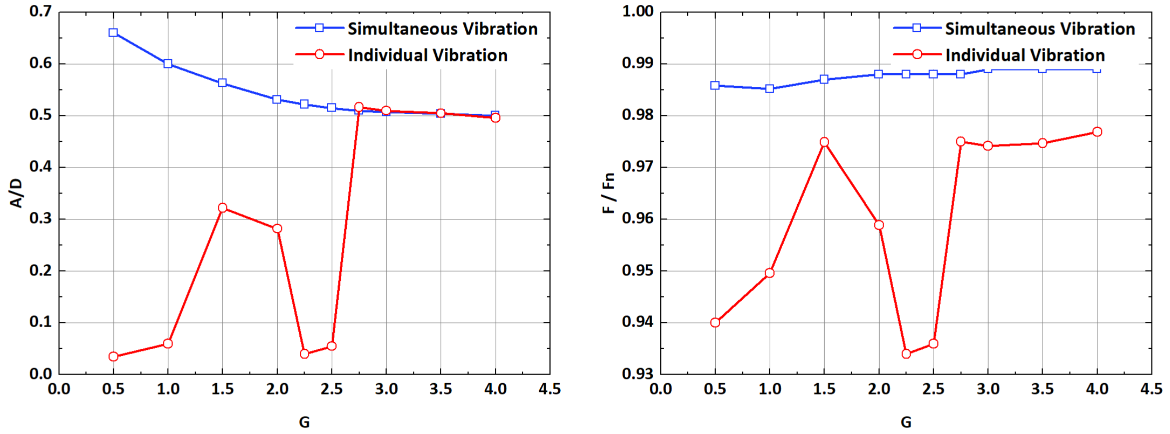

Figure 14 –Oscillation amplitude (left) and frequency ratio (right) of the plate in individual and simultaneous oscillation

Although the flat plate only vibrates for a specific range of G in the last part, it keeps vibrating for every configuration in simultaneous vibration, and its amplitude also increases gradually with the reduction of G. As shown in Figure 14, the maximum amplitude occurs for G=0.5D and reaches up to A/D=0.66 while it almost disappeared in the similar case of the last part. The frequency ratio behaves similar to the cylinder and follows the natural frequency.

The higher amplitude of both of the objects in simultaneous oscillation, especially in small horizontal spacing, shows that the present concept has a considerable potential to be utilized in the design of an improved energy harvesting system by converting fluid dynamic energy into electric energy from independent objects in a small area.

The phase difference between the motions of the two objects varies linearly and is a function of horizontal spacing. The maximum difference occurs for G=1D and in the case of G=3D two objects vibrate almost with the same phase (Figure 15).

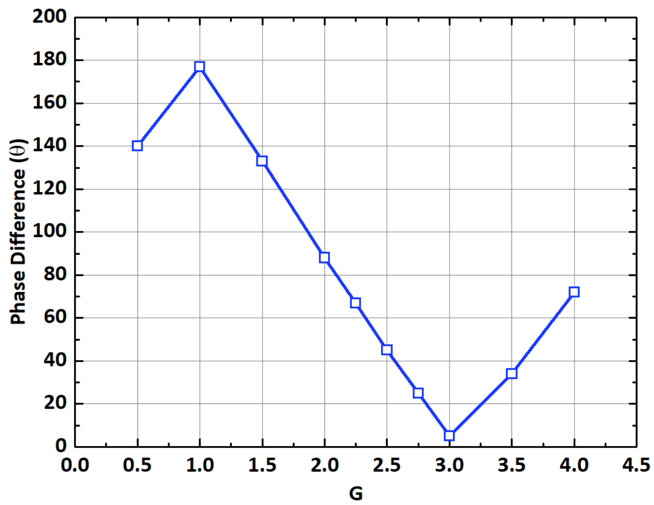

Figure 15 – The phase difference in oscillation of the circular cylinder and the flat plate in simultaneous oscillation

The CL_{rms} for both of the cylinder and the plate growth gradually as the plate gets closer to the cylinder (Figure 16).

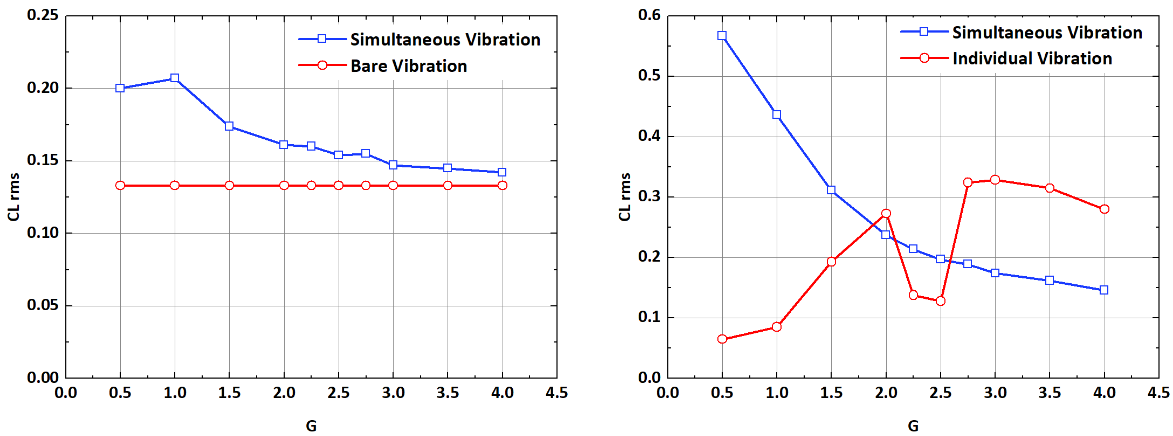

Figure 16 – CL_{RMS} of the circular cylinder (Left) and the flat plate (right) in simultaneous oscillation and bare or individual vibration

The higher value of CL_{rms} in small spacing is a result of change in lift force during one cycle of oscillation. As shown in Figure 17, not only the maximum lift coefficient rises about 20% for G=0.5D, but a secondary peak also appears in CL diagram just after the first one as the cylinder moves up or down (about 40%, 90% of a vibration cycle).

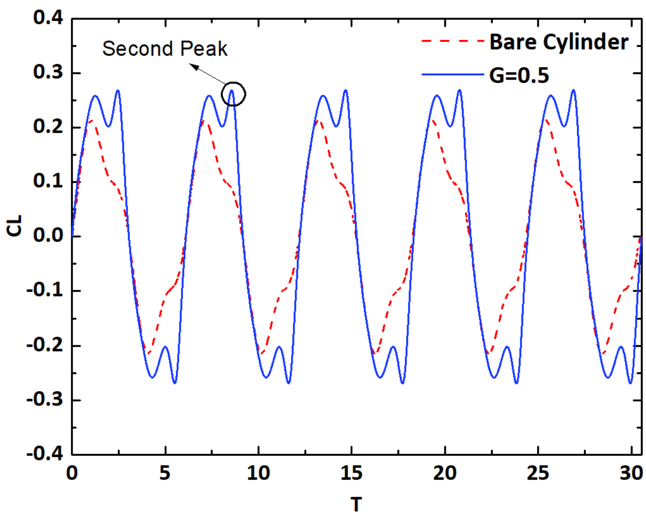

Figure 17 - Variation of Lift coefficient for the bare cylinder and in case G=0.5D

The Pressure Coefficient distribution also confirms the higher lift coefficient. The pressure difference on both of the front and rear side of the cylinder are slightly higher than that of a bare oscillating one (Figure 18).

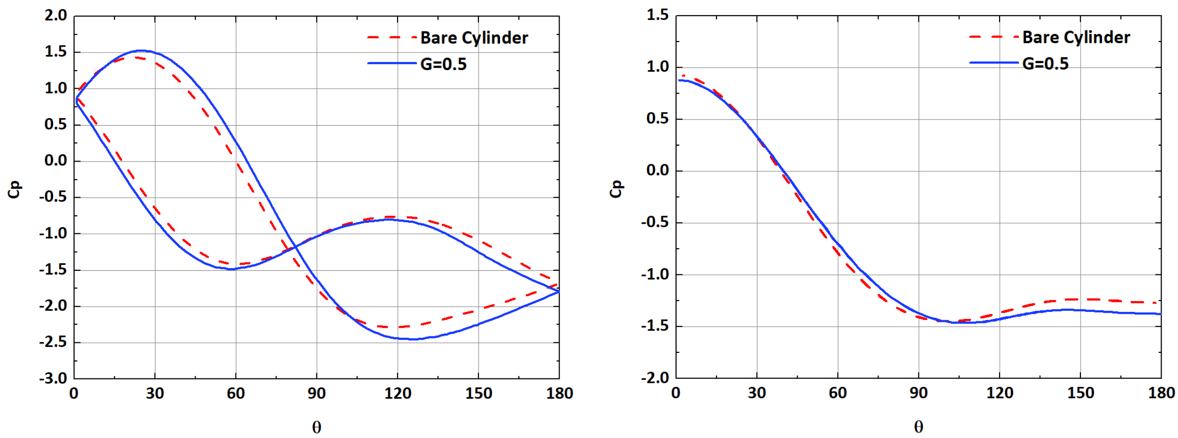

Figure 18 – Left) pressure coefficient on the circular cylinder for the bare one and in case G=0.5 at t=0.4T. Right) Time averaged pressure coefficient of the circular cylinder for the bare one and in case G=0.5D

Due to the change in shear layers and vortex formation, the time averaged pressure coefficient also shows a slightly higher pressure difference specially on the rear side of the cylinder in case G=0.5D. This change results in higher lift forces which is related to higher oscillation amplitude of this case (Figure 18).

To achieve a better understanding of how the flow field and the response of the system change, the vorticity contours for a bare cylinder and cases G=0.5, 3D are presented In Figure 19 for an identical moment ($Y_{cylinder}$=0).

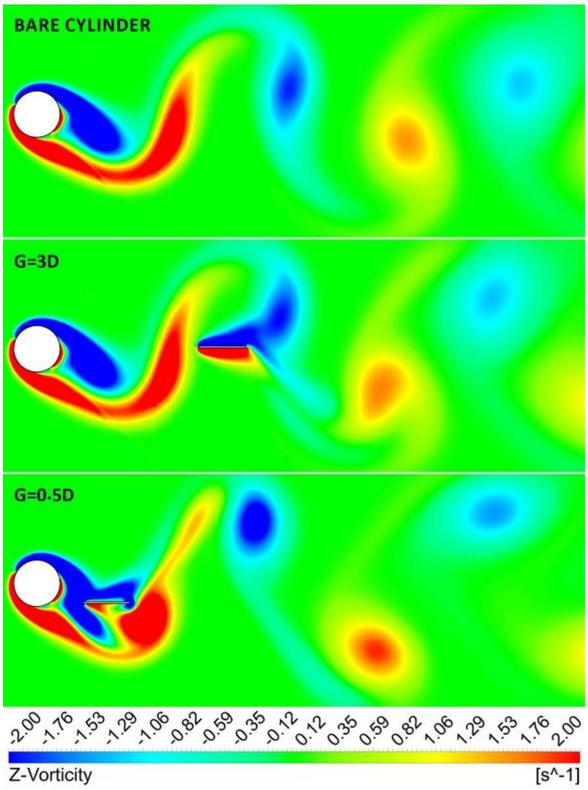

Figure 19 – Spanwise vorticity contours of the circular cylinder and the flat plate in simultaneous oscillation

Comparing the results shows a similar pattern for the case of G=3D and the bare one. The plate is far enough from the cylinder to form and shed the vortices, and has no significant effect on the upstream flow structure. In cases with low spacing (Ex. G=0.5D), the interaction of the flat plate and shear layers changes the vortex formation in such a way that increases the vortices strength and not only amplifies the cylinder oscillation amplitude but also lets the plate to oscillate with a considerable amplitude within such a short gap. Figure 20 presents the variation of the spanwise vorticity during one cycle of cylinder vibration at equal intervals.

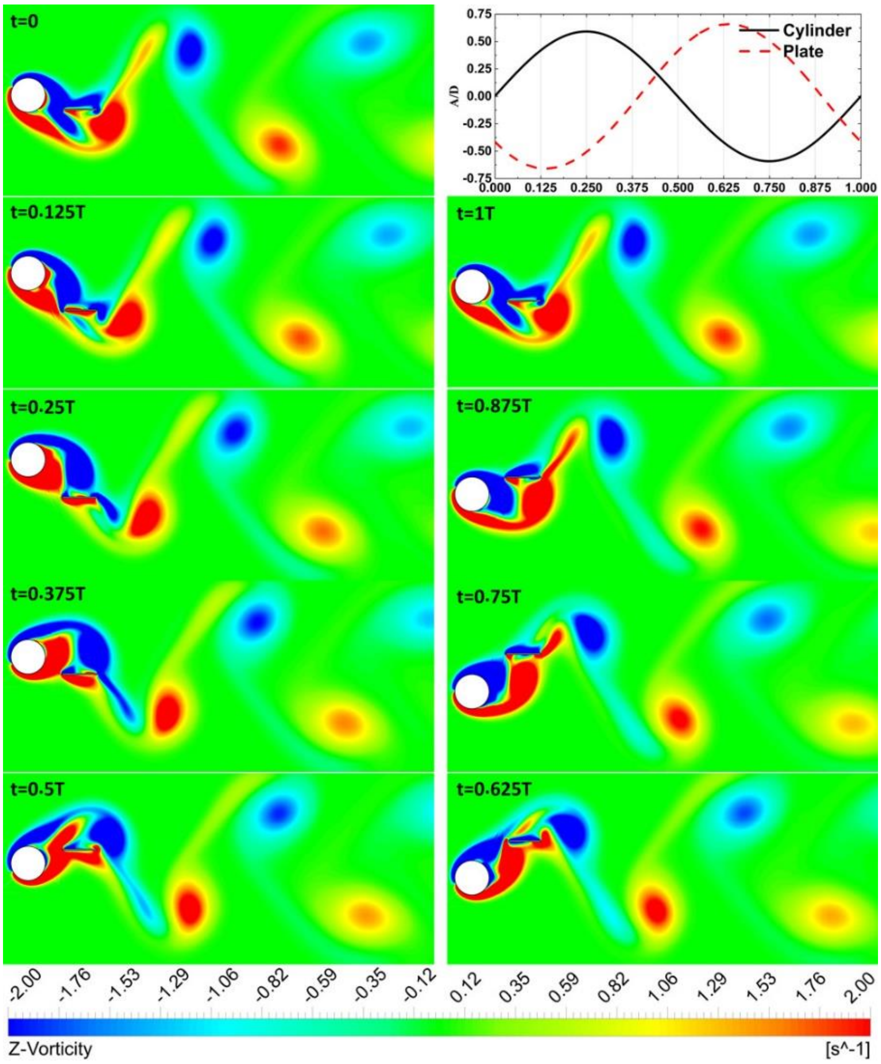

Figure 20 – Spanwise vorticity contours during one cycle of simultaneous oscillation for G=0.5D

The wake in this configuration is a bit different to that of a bare one. It is a bit wider, Vortices separate slightly sooner with a farther apart cores. They also have a long arm that is stretched toward the opposite side. The interaction between the plate, the shear layer, and forming vortex in each side of the plate, results in formation of a leading edge vortex (LEV) on the same side. The LEV extends and covers the entire plate surface and finally moves toward the trailing edge during one cycle of plate vibration. At this moment the second shedding vortex of the same side passes the plate, the TEV separates and joins the large vortex as its long arm.

Conclusion

Numerical simulations were conducted to investigate the effect of a free to vibrate flat plat on the wake structure and vortex induced vibration of an upstream circular cylinder in different horizontal spacing at a Re number of 100. The following major conclusions are drawn:

1. When the flat plate with one DOF in crossflow direction is placed beyond G=2.5D, just like a fixed one, has no considerable effect on the vortex formation and shedding of the cylinder. Therefore a regular wake forms and the plate starts to vibrate due to facing with an asymmetric flow domain.

2. Unlike the fixed one, placing the plate closer to the cylinder (G<2.6D), will not necessarily be associated with a delay in vortex shedding or suppression. According to the results, for a specific range of horizontal spacing (G=1.5, 2D), the plate starts to vibrate once again. Although its amplitude is less than the previous cases.

3. The cause of this phenomenon is attributed to the size of recirculation zone and the plate location. The flat plate starts to vibrate when it is completely, or at least a small part of it, located outside of the R-Z.

4. The plate starts to oscillate as facing with the upstream shedding vortices for cases with G≥2.75D. In those cases, as the shedding vortices move toward the plate, the asymmetric flow domain changes the flow field around the plate and induces a free vibration. The vibration mechanism is found different in cases of G=1.5, 2D. In these cases, although the most part of the plate is inside the R-Z, the vortices inside this region are smaller than those of G=2.5D and periodically move downstream and pass the plate. This flow structure results in a periodic pressure change, so the plate starts to vibrate.

5. In free simultaneous oscillation, the plate no longer plays the role of a splitter at any horizontal spacing. In large spacing, the flow structure around the cylinder is similar to that of a bare one and the cylinder and the plate start to vibrate due to VIV and WIV respectively.

6. As the plate gets closer, the oscillation amplitude for both of the objects increases gradually. This increment occurs due to the interaction of the plate and the shear layers which results in stronger vortices.

7. The higher amplitude in simultaneous oscillation, especially in small horizontal spacing, shows that the present concept has a considerable potential to be utilized in the design of an improved energy harvesting system from independent objects in a small area.

Acknowledgment

"The authors acknowledge the use of the UCL Grace High Performance Computing Facility (Grace@UCL), and associated support services, in the completion of this work."

References

[1] M. Armandei and A. C. Fernandes, “Marine current energy extraction through buffeting,” *Int. J. Mar. Energy*, vol. 14, pp. 52–67, 2016.

[2] T. Sarpkaya, “Vortex-induced oscillations: a selective review,” 1979.

[3] T. Sarpkaya, “A critical review of the intrinsic nature of vortex-induced vibrations,” *J. Fluids Struct.*, vol. 19, no. 4, pp. 389–447, 2004.

[4] P. W. Bearman, “Vortex shedding from oscillating bluff bodies,” *Annu. Rev. Fluid Mech.*, vol. 16, no. 1, pp. 195–222, 1984.

[5] C. H. K. Williamson and R. Govardhan, “Vortex-induced vibrations,” *Annu. Rev. Fluid Mech.*, vol. 36, pp. 413–455, 2004.

[6] A. Roshko, “On the drag and shedding frequency of two-dimensional bluff bodies,” 1954.

[7] J. H. Gerrard, “The mechanics of the formation region of vortices behind bluff bodies,” *J. Fluid Mech.*, vol. 25, no. 2, pp. 401–413, 1966.

[8] C. J. Apelt, G. S. West, and A. A. Szewczyk, “The effects of wake splitter plates on the flow past a circular cylinder in the range 104< R< 5× 104,” *J. Fluid Mech.*, vol. 61, no. 1, pp. 187–198, 1973.

[9] T. Adachi, T. Cho, K. Matsuuchi, T. Kawai, and H. Maeda, “The effect of a wake splitter plate on the flow around a circular cylinder,” *Trans. JSME*, vol. 56, no. 528, pp. 2225–2232, 1990.

[10] K. Kwon and H. Choi, “Control of laminar vortex shedding behind a circular cylinder

using splitter plates," *Phys. Fluids*, vol. 8, no. 2, pp. 479–486, 1996.

[11] S. Ozono, "Flow control of vortex shedding by a short splitter plate asymmetrically arranged downstream of a cylinder," *Phys. Fluids*, vol. 11, no. 10, pp. 2928–2934, 1999.

[12] J.-Y. Hwang, K.-S. Yang, and S.-H. Sun, "Reduction of flow-induced forces on a circular cylinder using a detached splitter plate," *Phys. Fluids*, vol. 15, no. 8, pp. 2433–2436, 2003.

[13] H. Akilli, B. Sahin, and N. F. Tumen, "Suppression of vortex shedding of circular cylinder in shallow water by a splitter plate," *Flow Meas. Instrum.*, vol. 16, no. 4, pp. 211–219, 2005.

[14] B. G. Dehkordi and H. H. Jafari, "On the suppression of vortex shedding from circular cylinders using detached short splitter-plates," *J. Fluids Eng.*, vol. 132, no. 4, 2010.

[15] H. Kawai, "A discrete vortex analysis of flow around a vibrating cylinder with a splitter plate," *J. Wind Eng. Ind. Aerodyn.*, vol. 35, pp. 259–273, 1990.

[16] Y. Nakamura, K. Hirata, and K. Kashima, "Galloping of a circular cylinder in the presence of a splitter plate," *J. Fluids Struct.*, vol. 8, no. 4, pp. 355–365, 1994.

[17] B. Stappenbelt, "Splitter-plate wake stabilisation and low aspect ratio cylinder flow-induced vibration mitigation," *Int. J. Offshore Polar Eng.*, vol. 20, no. 03, 2010.

[18] G. R. S. Assi and P. W. Bearman, "Transverse galloping of circular cylinders fitted with solid and slotted splitter plates," *J. Fluids Struct.*, vol. 54, pp. 263–280, 2015.

[19] J. Wu, C. Shu, and N. Zhao, "Numerical investigation of vortex-induced vibration of a

circular cylinder with a hinged flat plate," *Phys. Fluids*, vol. 26, no. 6, p. 63601, 2014.

[20] S. Liang, J. Wang, and Z. Hu, "VIV and galloping response of a circular cylinder with rigid detached splitter plates," *Ocean Eng.*, vol. 162, pp. 176–186, 2018.

[21] X. Sun, C. S. Suh, Z.-H. Ye, and B. Yu, "Dynamics of a circular cylinder with an attached splitter plate in laminar flow: A transition from vortex-induced vibration to galloping," *Phys. Fluids*, vol. 32, no. 2, p. 27104, 2020.

[22] H. Zhu, G. Li, and J. Wang, "Flow-induced vibration of a circular cylinder with splitter plates placed upstream and downstream individually and simultaneously," *Appl. Ocean Res.*, vol. 97, p. 102084, 2020.

[23] X. An, B. Song, W. Tian, and C. Ma, "Design and CFD simulations of a vortex-induced piezoelectric energy converter (VIPEC) for underwater environment," *Energies*, vol. 11, no. 2, p. 330, 2018.

[24] H. Wang, Q. Zhai, J. Hou, and L. Xia, "Numerical Investigation on the Vortex-Induced Vibration of a Flexible Plate behind a Circular Cylinder," *J. Coast. Res.*, vol. 85, no. sp1, pp. 1326–1330, 2018.

[25] M. L. Facchinetti, E. De Langre, and F. Biolley, "Coupling of structure and wake oscillators in vortex-induced vibrations," *J. Fluids Struct.*, vol. 19, no. 2, pp. 123–140, 2004.

[26] C. H. K. Williamson, "Vortex dynamics in the cylinder wake," *Annu. Rev. Fluid Mech.*, vol. 28, no. 1, pp. 477–539, 1996.

[27] C. H. K. Williamson, "Three-dimensional wake transition," in *Advances in Turbulence VI*, Springer, 1996, pp. 399–402.

[28] H. Jiang, L. Cheng, S. Draper, H. An, and F. Tong, "Three-dimensional direct numerical simulation of wake transitions of a circular cylinder," *J. Fluid Mech.*, vol. 801, p. 353, 2016.

[29] T. K. Prasanth, S. Behara, S. P. Singh, R. Kumar, and S. Mittal, "Effect of blockage on vortex-induced vibrations at low Reynolds numbers," *J. Fluids Struct.*, vol. 22, no. 6–7, pp. 865–876, 2006.

[30] T. K. Prasanth and S. Mittal, "Vortex-induced vibrations of a circular cylinder at low Reynolds numbers," *J. Fluid Mech.*, vol. 594, p. 463, 2008.

[31] T. K. Prasanth and S. Mittal, "Vortex-induced vibration of two circular cylinders at low Reynolds number," *J. Fluids Struct.*, vol. 25, no. 4, pp. 731–741, 2009.

[32] J. Park, K. Kwon, and H. Choi, "Numerical solutions of flow past a circular cylinder at Reynolds numbers up to 160," *KSME Int. J.*, vol. 12, no. 6, pp. 1200–1205, 1998.

[33] A. G. Kravchenko and P. Moin, "B-spline methods and zonal grids for numerical simulations of turbulent flows. Report No. TF-73, Department of Mechanical Engineering." Stanford University, 1998.

[34] J.-M. Shi, D. Gerlach, M. Breuer, G. Biswas, and F. Durst, "Heating effect on steady and unsteady horizontal laminar flow of air past a circular cylinder," *Phys. Fluids*, vol. 16, no. 12, pp. 4331–4345, 2004.

[35] S. Mittal, "Excitation of shear layer instability in flow past a cylinder at low Reynolds number," *Int. J. Numer. methods fluids*, vol. 49, no. 10, pp. 1147–1167, 2005.

[36] E. Stålberg, A. Brüger, P. Lötstedt, A. V Johansson, and D. S. Henningson, "High order accurate solution of flow past a circular cylinder," *J. Sci. Comput.*, vol. 27, no. 1–3, pp.

431–441, 2006.

[37] O. Posdziech and R. Grundmann, “A systematic approach to the numerical calculation of fundamental quantities of the two-dimensional flow over a circular cylinder,” *J. Fluids Struct.*, vol. 23, no. 3, pp. 479–499, 2007.

[38] Y. Li, R. Zhang, R. Shock, and H. Chen, “Prediction of vortex shedding from a circular cylinder using a volumetric Lattice-Boltzmann boundary approach,” *Eur. Phys. J. Spec. Top.*, vol. 171, no. 1, pp. 91–97, 2009.

[39] L. Qu, C. Norberg, L. Davidson, S.-H. Peng, and F. Wang, “Quantitative numerical analysis of flow past a circular cylinder at Reynolds number between 50 and 200,” *J. Fluids Struct.*, vol. 39, pp. 347–370, 2013.

[40] T. He, D. Zhou, and Y. Bao, “Combined interface boundary condition method for fluid–rigid body interaction,” *Comput. Methods Appl. Mech. Eng.*, vol. 223, pp. 81–102, 2012.

[41] J. Tu, D. Zhou, Y. Bao, J. Ma, J. Lu, and Z. Han, “Flow-induced vibrations of two circular cylinders in tandem with shear flow at low Reynolds number,” *J. Fluids Struct.*, vol. 59, pp. 224–251, 2015.